Preparation of functionally gradient ceramic membrane substrates

Darcovich, Kenneth; Price, M. E.

Journal of the Canadian Ceramic Society, 66, 2, 1997

PREPARATION OF FUNCTIONALLY GRADIENT CERAMIC MEMBRANE SUBSTRATES*

K. Darcovich+ and M.E. Price

ABSTRACT: A method for fabricating functionally gradient porous ceramic microstructures was conceived and investigated. Colloidally unstable or metastable suspensions of broad particle size distribution were prepared and slip cast to form ceramic discs. The suspensions were designed to promote segregation during consolidation and thereby produce the functionally gradient cross-section.

Preliminary results pertain to slip cast discs of α-alumina. A number of different size samples of alumina powder ranging in mean diameters from 0.2μm to 3.4μm were used to prepare the slips. Dispersing agents were ammonium salts of polymethylacrylic acid (PMAA). A number of experiments were conducted varying the particle size distribution of the powders in the slips, and the amount of polyelectrolyte along with pH control. Slurry solids content was also investigated as a means to control the rate of segregation which occurred in the consolidating slips. Finally the temperature profile of the sintering operation which the green bodies were subjected to contributed to the ultimate microstructure of the ceramic disc.

Ultimately it is desired to develop a process for making a substrate which is relatively tight-skinned on one side, thereby facilitating subsequent thin coating operations required for ceramic membrane making. Alternatively, the method can be refined to make microfiltration or ultrafiltration membranes in a single processing step.

Introduction

For the production of ceramic membranes, a porous ceramic support is typically used as a substrate prior to coating with a thin dense layer of additional ceramic material. Conventional ceramic support structures are not necessarily designed as membrane support substrates, rather they are simply marketed as "porous ceramics". They are typically made with monosized particles and have a uniform cross-section.

The present research investigates support structure preparation via a polydisperse slurry method, where the objective is to fabricate a functionally gradient material by a colloidal destabilization technique. The benefit of creating an asymmetric microstructure is to produce a smaller substrate pore size over a thinner region for a given bulk density.

The key for achieving asymmetry is to prepare colloidally unstable or metastable suspensions of a controlled and broad particle size distribution, encouraging segregation based on particle diameter to occur during consolidation. This produces a functionally gradient, or continuously finer mean particle diameter profile from bottom to top over the cross-section of the consolidated structure. The particle size distribution control is achieved by blending different powder samples. In terms of volume fraction, the continuous particle size distribution of the powder used to make the suspension should be coarse-rich. Preliminary results have confirmed the viability of this method.[1]

It has been shown that the colloidal state and suspension microstructure can be controlled with pH and polyelectrolyte stabilizing additives. The colloidal phase state of a suspension which forms the consolidated green body has a direct bearing on the eventual microstructure of the sintered solid object.[2,3] By controlling the dispersity of a suspension, slight aggregation and/or hierarchical clusters can contribute to overall porosity increases while the same time retaining a relatively fine pored top surface.

A general goal is to produce a structure (substrate) which should have a broader application than just an improved substrate for any or all subsequent coatings operations. Since this substrate is made functionally gradient by slip casting with a very broad particle size distribution, the resultant functionally gradient pore size distribution can achieve very small diameter pores at the top surface which extend to a relatively thin depth. This one-step processing method makes one contiguous solid entity, or substrate. With such a substrate it is possible to apply thinner defect-free membrane coatings than could be applied to conventional uniform microstructure substrates. To obtain a defect-free membrane, it is necessary to apply a thicker coating when the top surface of the substrate is composed of larger particles, contributing to larger pores and larger overall surface roughness.

A thinner coating (membrane) layer will achieve the same separation performance (based on membrane layer pore size distribution), but at a higher product rate, due to the lessened flow resistance, which is directly proportional to the membrane thickness. Naturally, a uniformly microstructured substrate can be made with very fines pores, but a significant expense in terms of permeate flux resistance. Further, a functionally gradient microstructure could eliminate the need for several intermediate layers which are often required for priming the substrate before the final membrane coating can be applied.[4]

Experimental

Seven α-alumina powders were available for this work. They were: Alcan C-84-LSB and C-82-LSB, Ceralox APA-0.2, APA-0.5 and HPA-1.0, and Sumitomo AKP-15 and

Institute for Chemical Process and Enviromental Technology, National Research Council of Canada, Ottawa, ON K1A 0R6.
* NRCC No. 37626
+Corresponding author.

AKP-30. These samples provided a particle size range from 0.06 to 70μm.

Particle Size Distribution

The particle size distributions of the seven powders were determined using a SediGraph 5000E Particle Size Analyzer, which is an x-ray sedimentation device operating in the Stokes regime and giving a cumulative mass percent distribution in terms of spherical diameter. Stable suspensions were prepared using Sedisperse A-12 dispersing agent as the liquid phase. Sedisperse A-12 is a highly purified, nonpolar, saturated aliphatic hydrocarbon of viscosity ≃ 4mPa/s, formulated for dispersing metal oxides. It is supplied by Micromeritics Instrument Corp., see the website **http://www.micromeritics.com/products/ps/5100/p33.htm** for further details

The cumulative particle size distributions of these powders are shown in Figure 1. Table 1 gives some additional data describing the powders. The values for specific surface area were taken from product technical information provided by the suppliers.

Suspension Preparation and Characterization

Alumina suspensions were prepared at solids loadings ranging from 5 to 40 v/o. The pH of these suspensions was controlled by small additions of concentrated HCl or NaOH and a steric effect was provided by the addition of an ammonium polyelectrolyte of molecular weight ≈ 15,000 (Darvan, C., R.T. Vanderbilt Co. Inc., Norwalk, CT), in accordance with a stability map.[5] The concentration of polyelectrolyte is expressed as mg/m^2, (i.e; mg polyelectrolyte per m^2 of alumina powder) determined from the powder specific surface areas given in Table 1. The extent of dispersion of a suspension of a given powder sample varies inversely with its viscosity. Viscometry measurements were made with a Bohlin VOR rheometer.

Drain Casting and Sintering

Preliminary tests were conducted to determine the effect of the processing variables, including solids concentration, on the quality of the consolidated ceramic pieces. Suspensions from 5 to 40 v/o were drain cast in 45 mm tubular moulds over gypsum slabs to green thicknesses from 4 to 7 mm. Depending on the grain size, sintering was performed at the lowest possible temperature (≈ 10 hours ramp and soak cycle, 1150 to 1400°C maximum temperature) to achieve a slight amount of fusion to strengthen the body and immobilize the ceramic particles, while retaining as much porosity as possible. A time profile schematic is shown in Figure 2.

powder	d_{50} μm	d_{10}-d_{90} μm	distribution characteristic	specific surface area (m^2/g)
AKP-30	0.20	0.09 - 3.64	narrow	8.6
APA-0.5	0.45	0.31 - 0.66	narrow	8.1
HPA-1.0	0.68	0.35 - 2.50	narrow	4.4
AKP-15	0.71	0.40 - 1.30	narrow	2.5
C-82-LSB	0.86	0.35 - 8.71	broad	4.0
C-84-LSB	1.33	0.51 - 6.32	broad	6.0
APA-0.2	3.73	0.40 - 9.79	broad	40.0

Table 1 Powder size distribution properties

Hardness Testing

To investigate cross-sectional properties of the samples, Vickers Hardness (with 10 kg weight) and microhardness tests (with 300 g weight) were performed. Hardness testing was chosen because of the relative reliability of the results as compared to tensile or compression tests in which the strength of a ceramic is highly dependent on imperfections in the specific sample.

A total of eight samples were prepared and sintered at regular intervals from 1000°C to 1300° C. Four samples expected to give uniform cross-sections (AKP-15, 10 v/o, pH =2, no polyelectrolyte added), were compared to samples expected to form functionally gradient microstructures (C-84-LSB, 10 v/o, pH=5.6, polyelectrolyte concentration of 1.0 mg/mg^2).

To perform the tests, the alumina discs were sectioned with a diamond saw, cold mounted (Beuhler Ultra-Mount epoxy), leveled and then polished. The final finish was done with 600-grit sandpaper under running water.

A matrix of identations was made with a diamond microtip over the cross-section of each sample. The dimensions of the indents were then determined using a microscopic image

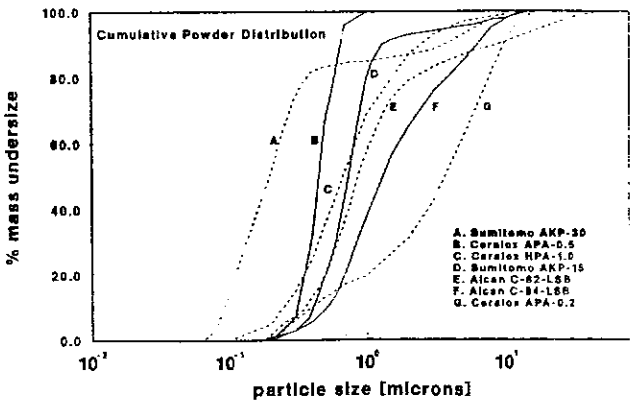

Fig. 1 Cumulative mass distributions of the alumina powder samples.

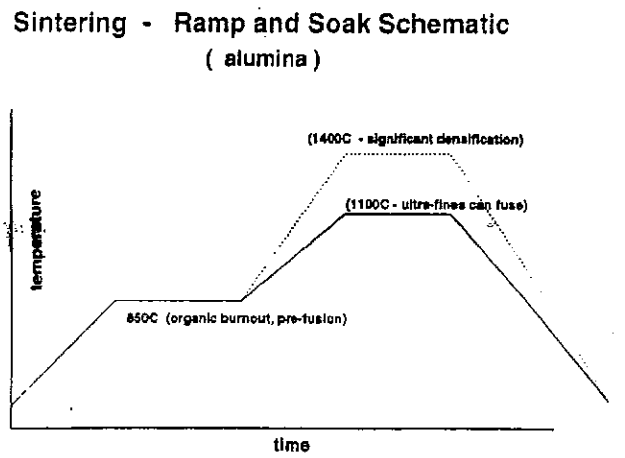

Fig. 2 Schematic ramp and soak sintering profile.

analysis system. The Vickers Hardness Numbers, H, were calculated as:

$$H = \frac{1.8544M}{d^2}$$

where M is the mass acting on micro-tip (kg) and d is the diagonal length of the indent (mm).

Results and Discussion

A number of processing variables known to affect the properties of the eventual sintered body were considered in experiments. These included the solids concentration, the particle size distribution, colloidal stabilization agents (pH, polyelectrolytes) and the sintering ramp and soak profile. Some quantities were measured in order to characterize the ceramic. These were suspension viscosity, bulk density and hardness.

Suspension Microstructure

Interparticle interaction forces control the state of dispersity of sub-micron alumina suspensions. The nature of these interactions can be estimated by applying DLVO theory to the suspensions, to estimate the extent of interparticle attraction or repulsion at work.[6] A rigorous quantitative analysis was not considered to be essential for this discussion. The general guiding principles resulting from DLVO theory can be summarized by stating that interparticle repulsive forces will come from surface electrical charges and electrosteric effects from adsorbed polyelectrolytes, all modified by pH and ionic strength. Attractive forces between particles will be the downward gravitational force and van der Waals body forces. With an isoelectric point for α-alumina around pH=9,[7] and heightened polyelectrolyte activity occurring at pHs less than this,[5] metastable states might be expected to exist at pHs less than 9.

Figure 3 shows viscosities across a pH range, measured from 30 v/o suspensions of AKP-15 alumina, taken at a shear rate of 116 s^{-1}. It can be seen that between pH 6 and 9, the viscosity increases nearly two orders of magnitude for the cases where no polyelectrolyte is present to provide any steric stabilization. At pHs above 6, a polyelectrolyte concentration of 2.0 mg/m^2 was able to maintain the suspension viscosities at a level comparable to the electrostatically stabilized cases. The zeta potentials for the purely electrostatic cases in this pH range are quite low. The polyelectrolyte absorption occurring at high pH has almost complete functional group dissociation, thereby achieving a surface charge reversal, imparting good steric stability to the suspensions, reflected by the low viscosity measurements.[8]

For the low pH cases, charge neutralization occurs by polyelectrolyte adsorption at pH 4, destabilizing an otherwise electrostatically stable suspension. At pH 2 the 2.0 mg/m^2 polyelectrolyte suspension has a higher viscosity than the one made with only 1.0 mg/m^2. In this case more polyelectrolyte is available to neutralize an even greater positive surface charge, and the polyelectrolyte concentration may be high enough to allow any excess to remain in the aqueous phase, thereby increasing its viscosity. From the results in Figure 3, metastable states can be expected between pH 4 and 6, with some addition of polyelectrolyte.

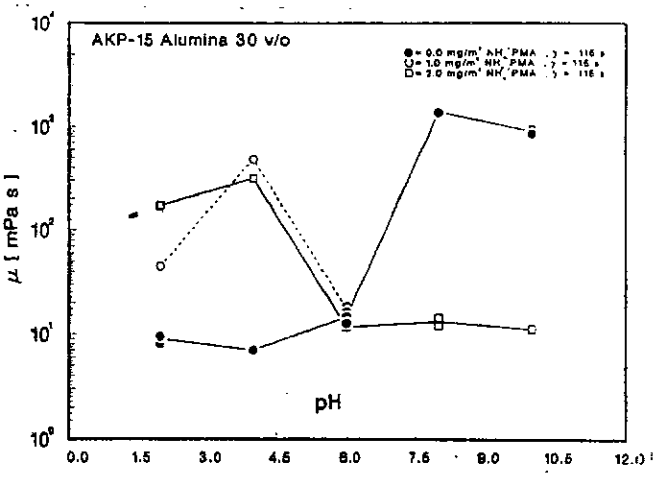

Fig. 3 Suspension viscosity versus pH with polyelectrolyte dosage as parameter.

Green Body Consolidation and Sintering

An objective was to exploit system parameters controlling relative sedimentation rates to promote the formation of a functionally gradient microstructure. Stokes' Law predicts the sedimentation rate, v, for a single particle of diameter d and density ρ_s, settling in an infinite fluid medium of density ρ_f and viscosity μ_f.

$$v = \frac{d^2(\rho_s - \rho_f)g}{18\mu_f}$$

Fluid viscosity, fluid density and solid density can all be adjusted to influence the overall sedimentation rate. The particle diameters, determined by controlling the particle size distribution can be exploited to control relative sedimentation rates and achieve a functionally gradient microstructure. Larger particles will settle more rapidly than small ones. With a broad and continuous particle size distribution, a continuously finer microstructure can be formed from bottom to top in the consolidated body.

The samples were sintered under temperature profiles as shown in Figure 2. The densities of the sintered bodies were estimated by averaging a number of thickness and diameter measurements made with precision calipers.

The 10 v/o suspensions over a variety of conditions appeared to make the most uniform and smooth consolidated disks. In all cases, it was clear from simple visual inspection that the top layer was smoother (finer grained) than the bottom layer. SEM analysis of the cross-sections showed a grain-sized based asymmetry in the samples, more pronounced at pH 5, where the colloidal stability of the suspension was compromised.[1]

Hardness Measurements

A series of experiments was conducted to try to show a difference between sintered bodies formed from colloidally stable and uniform suspensions, and bodies formed from colloidally metastble and polydisperse suspensions. Figure 4 shows hardness profiles measured on the samples meant to

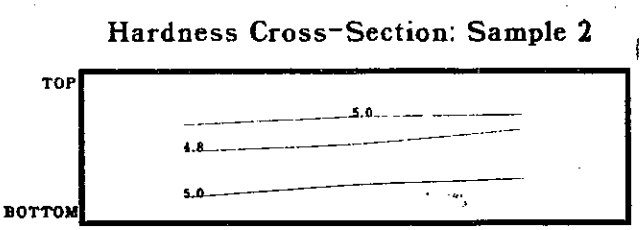

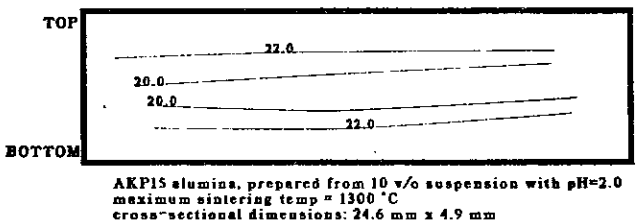

Fig. 4 Cross-sectional hardness profiles for samples prepared with narrow particle size distribution in colloidally stable regime. No polyelectrolyte added.

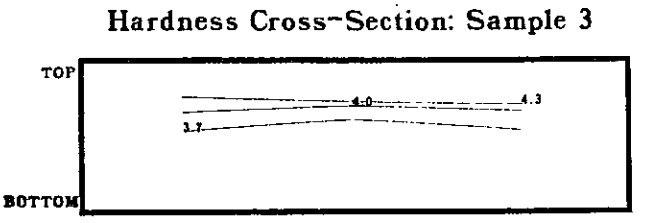

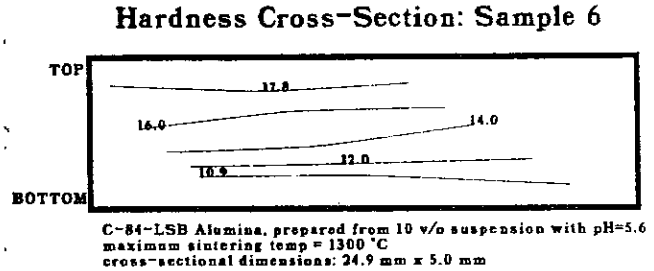

Fig. 5 Cross-sectional hardness profiles for samples prepared with broad particle size distribution in colloidally metastable regime. 1.0 mg/m² polyelectrolyte concentration.

be stable and uniform (See section on Hardness Testing). The variation of the hardness from the center to the edges was between 4 and 10%, likely due to heat conduction restrictions during sintering. There was no discernible cross-sectional trend aside from this for these samples. The samples prepared from the metastable and polydisperse suspensions show a definite asymmetry in their hardness profiles, shown in Figure 5.

For the 1000°C and 1300°C cases given in Figures 4 and 5, the structure made from the AKP-15 powder were found to be harder. This would indicate a more fully fused microstructure, a result of sintering with a smaller mean particle diameter. Further, the AKP-15 powder has a narrow particle size distribution, which inhibits grain growth giving more uniform sintering which translates to higher strength or hardness. Naturally, the hardness increased with sintering temperature, an indication of the densification taking place, as well as the degree of particle fusion forming a continuous solid piece. The hardness determined here were in the 5 to 20 kg/mm^2 range. The green bodies were too soft to produce any reliable hardness data with the indenting weights used. A four-fold increase in hardness indicates increasing densification as the sintering temperature was raised. The measured sample values are quite low compared to fully dense alumina, which has a hardness of around 2000 kg/mm^2 at ambient temperatures.[9] The absolute hardness values are low due to the high porosity of the samples and the weak neck regions which would be formed at these relatively low sintering temperatures.

Sintered Microstructure

The polydispersity of the powders may bring about a situation where the fine grains sinter locally and form a strengthened structure without visible linear shrinkage in the bodies. Interparticle forces determined by DLVO theory suggest that with metastable conditions, attractive potentials will first exist between the smallest particles and the largest particles of a distribution. (Please refer to the appendix for quantitative details demonstrating this condition). That is, with a broad particle size distribution, the metastable conditions will spread the finest material throughout an otherwise functionally gradient microstructure. These fines are sinterable at lower temperatures and act as localized bonding sites, in every part of the structure. The bottom, or coarse sections of the functionally gradient microstructures would hot harden much at low-end sintering temperatures without the presence of fines to create spot joints. A similar study for the purpose of producing porous refractories referred to such fine particles as "active", and depending on their size, sintering could occur at a temperature as low as 1000°C.[10]

Figure 6 is a plot of sintered density versus temperature, as well as the median hardness for these same samples versus temperature. Naturally, the density (which corresponds inversely to the porosity) and the hardness increase with sintering temperature. However, a closer examination of these curves reveals some interesting results. The broad particle size distribution, which might otherwise be expected to pack more densely, gave a lower density when consolidated from a metastable suspension than the narrow particle size distribution powder consolidated from a stable suspension. Clustering effects and site sintering of fines could contribute to a high porosity for the functionally gradient microstructures. This concept is supported by the median hardness curves also shown in Figure 6. At 1200°C the functionally gradient structure had roughly the same porosity as the uniform structure, yet the hardness was almost double. This suggests that the slight dispersal of fines inside the consolidated structure would have acted as local sintering sites, strenthening the body without significantly densifying it. By 1300°C, the uniform microstructure shows a higher hardness and density. Its more regular particle packing coupled with a smaller mean grain size allowed a greater amount of sintering to occur,

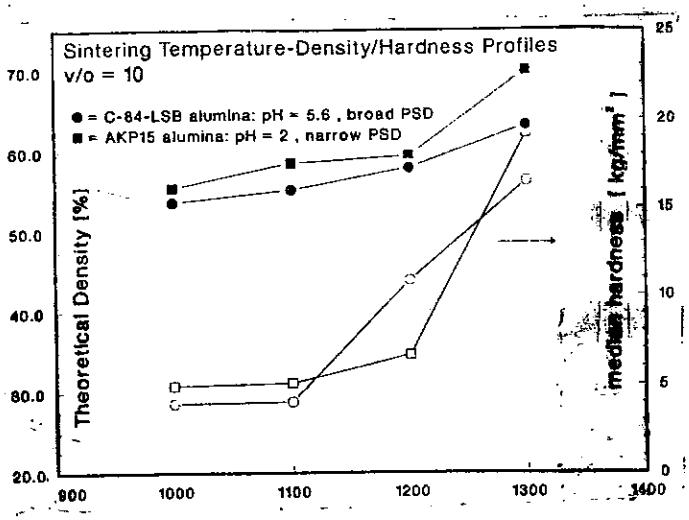

Fig. 6 Plot of sintered density versus sintering temperature for uniform and functionally gradient microstructures. Also median hardness versus sintering temperature.

contributing to the high density and hardness. Another study on the effects of the powder properties on the formation of microfiltration membranes showed that when agglomerate containing bodies were sintered, powder densification occurred within agglomerates and the degree of densification of membrane structure is slower than in well dispersed bodies[11]. These agglomerate containing bodies were also found to exhibit larger pore sizes than well dispersed samples, although no attempt was made to design any functionally gradient character into the microstructures to produce a finely pored top surface.

Some initial porosimetry data indicate top layer pore sizes of under 0.05 μm for the functionally gradient microstructures, putting them in the ultrafiltration regime as filter materials. Further, the pore size distribution was broad, corresponding to a functionally gradient microstructure.

Summary and Conclusions

Initial results show that metastable slurries of broad particle size distribution alumina form functionally gradient or continuously asymmetric porous microstructures. Metastable slurries were considered to have viscosities in the transition region between low and high values, at a pH and polyelectrolyte concentration where partial electrostatic charge neutralization will have occurred. Samples prepared at pH=5.6 and 1.0 mg/m^2 polyelectrolyte concentration were considered to be metastable. Slip casting with a broad particle size distribution and under colloidally metastable conditions can enhance porosity and produce a functionally gradient microstructure with a very fine top layer in one step. Differential sedimentation rates of particles within the broad particle size distribution produce a consolidated green body with said functionally gradient microstructure. Data suggest that there is a slight dispersal of fines inside the consolidated structure which act as local sintering sites, strengthening the body without excessive densification. Sintered density and hardness data for both uniform and functionally gradient samples support this concept. With preliminary porosimetry data, top layer pore sizes of under 0.05 μm are in the ultrafiltration regime. Such structures could be used as ultrafiltration membranes directly, or as substrates for applying thin coats of finer material to produce membranes for reverse osmosis or gas separation. Reducing the number of intermediate coating layers to achieve to top layer pore size of a desired fineness should be facilitated with these functionally gradient structures.

The initial success in producing a functionally gradient microstructure with metastable polydisperse suspensions poses a number of research questions for further refining the procedure. To this end future work will involve carrying out a multi-variable factorial experimental design to determine interdependent effects among processing variables. One response in this analysis will come from porosimetry measurements, giving porosity and pore size distributions.

A module to house the structures is currently being constructed, and will become available for permeation testing.

A future goal is to use these structures as substrates for thin film membrane coatings, and to conduct separations tests.

Acknowledgements

The authors gratefully acknowledge Mr. Dave Morphy of NRC-IAR for his assistance with the hardness measurements, and Mr. Garry Polomark of NRC-IRC for his assistance with the particle size distribution measurements.

Appendix

A calculation can be made to determine DLVO interaction potentials for the range of possible particle-particle pairs in the distribution of the Alcan C-84-LSB powder sample to show which pair combinations are most liable to associate.

A numerical integration of the mass frequencies of each radius, f(r), across the particle size distribution in Figure 1 for C-84-LSB will provide a number count N_{TOT}, of particles per gram of sample.

$$N_{TOT} = \int_{r_S}^{r_L} \left(\frac{f(r)}{\rho \frac{4}{3}\pi r^3} \right) dr$$

Using a 15-point Gaussian quadrature routine (IMSL:QDAG), a value for N_{TOT} of 2.42 x 10^{12} particles per gram was determined. With the density of α-alumina at 3.96 g/cm^3,a mean radius of 0.292 μm results.

At 10 v/o, a shell volume per particle is determined as 0.630 μm. The mean interparticle separation, h, is thus,

$$h = 2(r_{shell} - \bar{r}) = 6.759 \times 10^{-7} m$$

A DLVO interaction potential, V_T, can be calculated for two spheres of diameters a_1 and a_2 according to formulae given in.[6] V_T contains an attractive potential V_A, and a repulsive component V_R, so that $V_T = V_R + V_A$.

For two interacting spheres of diameters a_1 and a_2,

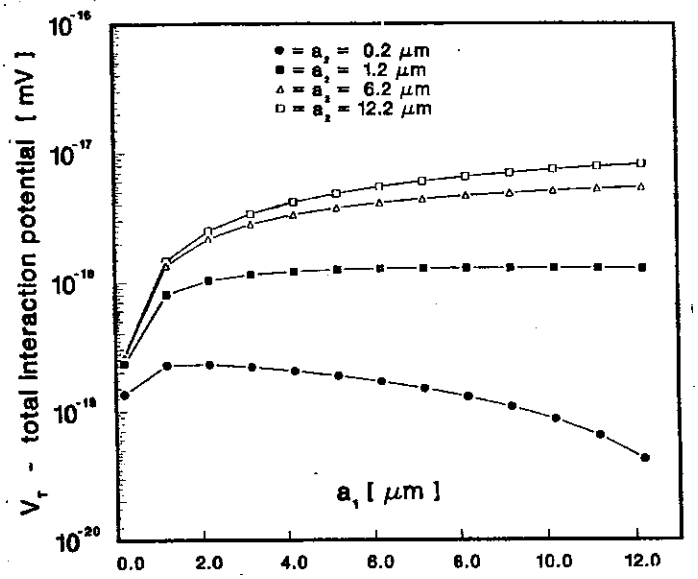

Fig. 7 The total interaction potential for the range of possible a_1 - a_2 diameter combinations of C-84-LSB powder under metastable suspension conditions.

$$V_R = \frac{64\pi\varepsilon a_1 a_2 k^2 T^2 \gamma_1 \gamma_2}{(a_1 + a_2)e^2 z^2} \exp[-\kappa h]$$

Above,

$\varepsilon = 78.5 \times 8.854 \times 10^{-12}$ [F/m]	medium dielectric constant
$k = 1.3805 \times 10^{-23}$ [J/K]	Boltzmann's constant
T = 293 [K]	temperature
$e = 1.602 \times 10^{-19}$ [C]	elementary change
z = 1 [dimensionless]	ionic charge number

The quantity γ_i is given by,

$$\gamma_i = \frac{[ze\xi_i / 2kT] - 1}{[ze\xi_i / 2kT] + 1}$$

where ξ_i is the zeta potential of the ith dispersed particle [mV]. For the metastable state under consideration, we set $\xi \simeq -5.0$ mV. To calculate κ[1/m] (inverse double layer thickness) we use,

$$\kappa = \left(\frac{4e^2 N_A I}{\varepsilon kT}\right)^{\frac{1}{2}}$$

where, N_A is Avogadro's number equal to 6.203×10^{23} [mol^{-1}], and I is the ionic strength of the counter-ion. $I = \frac{1}{2}\Sigma c_i z_i^2$ where c is in [mol/m^3].

For V_A we have,

$$V_A = \frac{-A}{12}\left[\frac{y}{(x^2 + xy + x)} + \frac{y}{(x^2 + xy + x + y)} + 2\ln\left(\frac{x^2 + xy + x}{x^2 + xy + x + y}\right)\right]$$

where,

$$x = \frac{h}{a_1 + a_2} \text{ and, } y = \frac{a_1}{a_2} (y > 1)$$

A is the Hamaker constant, equal to 8.6×10^{-20} [J].[7]

The attractive potential V_A is a negative quantity, and if it dominates, the next interaction V_T will be negative. Very low positive values of V_T are sufficient to bring about flocculation. Figure 7 shows V_T plotted against the particle size range (a_1) of the C-84-LSB powder, with four curves representing four different values of a_2. It can be seen that the lowest value of V_T occurs at $(a_1,a_2) = (12.2,0.2)$, or as stated in the section on Sintered Microstructure, between the smallest and largest particles of the distribution. Further , the interaction potential across most of the range of particle sizes is at a minimum with the smallest particle. That is, flocculation is energetically favoured to first occur for these particles with the smallest particles.

References

1. Darcovich, K. and Price, M.E., "Microstructure Processing for Asymmetric Ceramic Membrane Substrates", in Proceedings of the International Membrane Science and Technology Conference - IMSTEC'96, Sydney, Australia, Nov. 12-14, 164-166, 1996.
2. Aksay, I.A., "Microstructure Control Through Colloidal Consolidation", In: Advances in Ceramics, v.9, J.A. Manjels and G.L. Messing (eds.), 94-104, 1984.
3. Lamas, A.G., Almeida, M., and Diz, H.M.M., "Slip Casting of Alumina Bodies With Differential Porosities", *Ceram. Int.*, **19**, 121-124, 1993.
4. Maebashi, N., "Ceramic Membranes and Application to the Recovery of Soy Sauce", in Porous Materials, K. Ishizaki (ed.), 81-87, 1993.
5. Cesarano (III), J., and Aksay, I.A., "Processing of Highly Concentrated Aqueous α-Alumina Suspensions Stabilized With Polyelectrolytes", *J. Am. Ceram. Soc.*, **71** [12], 1062-1067, 1988.
6. Shaw, D.J., Introduction to Colloid and Surface Chemistry, 4th ed., Boston: Butterworth-Heinemann, 1992.
7. Bergström, L.,"Surface Chemical Characterization of Ceramic Powders", In: Surface and Colloid Chemistry in Advanced Ceramics Processing, R.J. Pugh and L. Bergström (eds.), 71-125, 1994.
8. Cesarano (III), J., Aksay, I.A., and Bleier, A.,"Stability of Aqueousα-Al_2O_3 Suspensions with Poly(methacrylic acid) Polyelectrolyte", *J. Am. Ceram. Soc.*, **71** [4], 250-255, 1988.
9. Dörre, E. and Hübner, H., *Alumina*, Berlin: Springer-Verlag, 1984.
10. Franklin, S.A. and Rand, B., "Partial Sintering in Porous Alumina Refractories: Effect of Size Distribution on Microstructure and Elastic Modulus", *British Cer. Trans.*, **95** [3] 93-98, 1996.
11. Levänen, E., Kolari, M. and Mäntylä, T., "The Effect of Raw Material Powder on the Properties of Alumina Microfiltration Membranes", in *Ceramics*: Charting the Future, P. Vincenzini, (ed.), **3**, 2755-2762, 1995.